Theoretical Consideration on Influences of Cavity or Pillar Shape on Band Structures of Silicon-Based Photonic Crystals

Yoshifumi OGAWA, Issei TAMURA, Yasuhisa OMURA, and Yukio IIDA

(Received September 12, 2005)
(Accepted January 30, 2006)

Abstract

This paper describes the physical manifestations of the various influences of cavity (or pillar) shape and the filling factor of dielectric material on band structures in two-dimensional photonic crystals. The influences of circular or rectangular cross-sections of cavity (or pillar) arrays on photonic band structures are considered theoretically, and significant aspects of square and triangular lattices are compared. It is shown that both the averaged dielectric constant of the photonic crystal and the distribution profile of photon energy play important roles in defining optical properties. For the triangular lattice, especially, it is shown that cavity array with a rectangular cross-section breaks the band structure symmetry. So, we go on to discuss this from the perspective of band structure, and consider the optical properties of a lattice with a circular cross-section cavity.

1. Introduction

The increasing scale of integrated Si devices has given rise to a significant increase in the signal delay time between circuit blocks; the signal delay time is now much longer than the gate delay time of individual devices. It was expected that this difficulty could be overcome by an advanced metallization technique that replaces Al-based wires with Cu-based wires and the SiO_2-based interlayer dielectrics with a low-k dielectric material. However, it is anticipated that the propagation delay time of signals through interconnections will still determine the speed of integrated circuits when the gate length falls below 0.18 μm. This problem may be overcome by setting optical links between circuit blocks in a chip or LSIs to transfer signals. Silicon-based waveguides have been widely studied from the viewpoints of monolith circuits and process compatibility [1]. The designs must allow for problems such as sharp bends, mode dispersion, and specific attenuation.

Against this background, photonic crystal (PC) materials are attracting attention for controlling light wave transmission [2-4]; photonic band-gap (PBG) structures are especially useful in applications where the spatial localization of light waves is required [5]. In a three-dimensional (3-D) PC, we can control the propagation of light waves in all directions. Generally speaking, however, it is very difficult to fabricate 3-D PC structures. Its simpler cousin, 1-D PC, offers significantly easier fabrication at the cost of reduced functionality. Recently, the influence of defects in 1-D PC waveguides with periodic air cavities has been demonstrated experimentally, and the characteristics of such waveguides have been

examined by simulations [6]. However, it has been clarified that design parameters, such as the shape and dimensions of the air cavities, significantly affect the characteristics of the 1-D PC waveguide [7].

On the other hand, a two-dimensional (2-D) photonic crystal appears to have a high potential for light-beam control capability, and it has attracted much attention [8-21]. Since 2-D photonic crystal has a flexible photonic band structure, the propagation of light waves can be controlled using the 2-D PC [1, 2]. In addition, in some cases, the PC gives a specific restriction to light-wave propagation even out of PBG: super-prism, self-collimation and super-lens are typical phenomena [9-12]. These phenomena suggest higher potential applications of the PC for information processing. For these reasons, the 2D PC has been widely investigated. From the point of view of physics-based consideration, the pillar or cavity array with a circular or rectangular cross-section has been investigated extensively [13, 14] because pillar shapes influence the dispersion relation of light-wave propagation.

In this paper, we will categorize aspects of the optical properties of the PC consisting of square lattice or triangular lattice with a circular or rectangular cross-section of pillar or cavity. We will also address specific features of the triangular lattice because of breaks in propagation symmetry.

2. Periodic Cavity Array

We will consider two kinds of lattice structures: square lattice and triangular lattice. As is well-known, these lattices show quite different photonic band structures. Perfect band gap is created for triangular lattices. In the following sections, photonic band structures of lattices with air cavity array and pillar array are considered. In the simulations, two-dimensional lattices are assumed. Band structures are calculated by the orthogonal plane wave expansion (OPW) method, and the photonic band structures are obtained by resolving with 225-plane waves [3].

2. 1 Square lattice

Let us consider the photonic bands of an air cavity array in silicon. A square lattice with air cavities, whose cross-sections are circular or rectangular is shown in Fig. 1. The periodic cavity array is assigned in x-y plane. It is assumed that material is uniform along the z direction. In Fig. 1, **a** is the lattice constant, **r** is the radius of cavity having a circular cross-section, **d** is the width of rectangular cavity. We calculate the dispersion relations of these photonic crystals for various **r/a** or **d/a** values. Fig. 1(a) shows the photonic band gap (PBG) map for a square lattice in which the cross-section of the air cavity is circular. The vertical axis shows the normalized frequency (ω**a**/2π**c**), where c is the light wave velocity. The horizontal axis shows the circular radius normalized by the lattice constant (**r/a**). In the photonic band gap map, the gray zone shows the photonic band gap for the TE wave (magnetic field is parallel with the direction of depth of air cavity). Inside the gray zone, regardless of crystal axis, the TE wave does not propagate. The black zone shows the photonic band gap for the TM wave (electric field is parallel with the direction of depth of

air cavity). Inside the black zone, the TM wave, regardless of crystal axis, does not propagate. The dark gray zone shows the perfect photonic band gap, in which any light wave mode does not propagate. The band gap for the TE wave and that for the TM wave partly overlap as seen in Fig. 1(a).

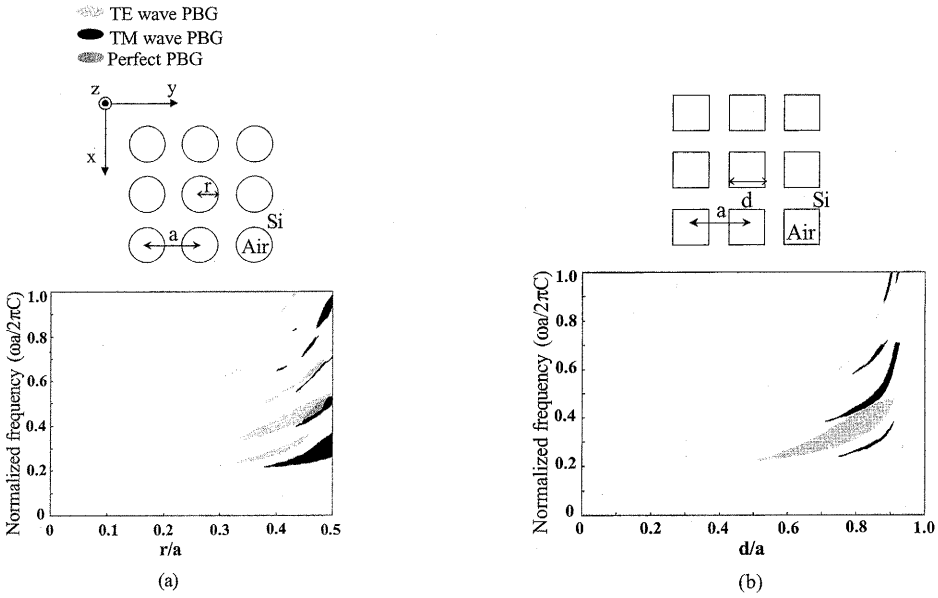

Fig.1 Photonic band gap (PBG) map for various square lattices.
(a) Circular cross-section of cavity
(b) Rectangular cross-section of cavity

Fig. 1(b) shows the PBG map for a square lattice in which the cross-section of the cavity is rectangular. In Fig. 1(b), the horizontal axis shows a width of rectangular cavity normalized by the lattice constant **(d/a)**. Comparing features of the two photonic band-gap maps, the photonic band gap of TE wave for the lattice with a rectangular cross-section is wider than that for the lattice with a circular cross-section, and the photonic band gap of TM wave for the lattice with a rectangular cross-section is narrower than that for the lattice with a circular cross-section. The perfect photonic band gap shares a limited zone for the lattice with a circular cross-section (See Fig. 1(a)). Here we define the filling factor **(f)** which denotes the ratio of cavity cross-sectional area to unit cell area; $\mathbf{f=\pi r^2/a^2}$ for the circular cross-section and $\mathbf{f=d^2/a^2}$ for rectangular cross-section. At a small filling factor **(f)**, we can see little difference in band structures between these two cavity shapes.

Figs. 2(a) and 2(b) show dispersion relations for the square lattice with a circular cross-section **(r/a=0.17** in Fig. 2(a)) and the square lattice with a rectangular cross-section **(d/a=0.30** in Fig. 2(b)). The values of **r/a** and **d/a** are taken so that the filling factors of these two lattices are identical to each other **(f=0.09)**. Since f value is so small, the difference of dispersion relations is not significant. The lattice shape does not influence the band structure because of small volume of cavity. We also examined whether the filling factor has in a very slight influence on dispersion relations for $\mathbf{f < 0.16}$.

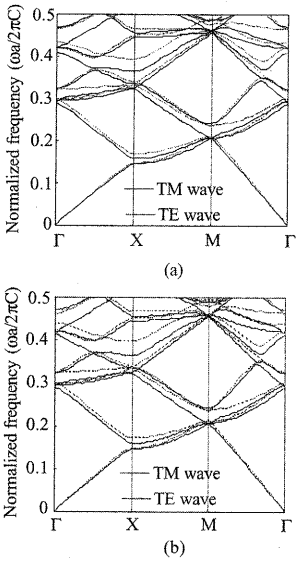

Fig.2 Dispersion relations for various square lattices (**f=0.09**). Solid lines are for TM waves and broken lines for TE waves.
(a) Circular cross-section of cavity (**r/a=0.17**).
(b) Rectangular cross-section of cavity (**d/a=0.30**).

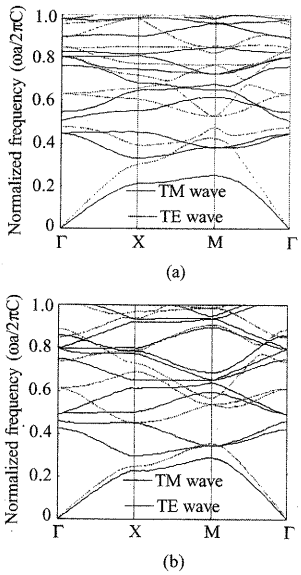

Fig.3 Dispersion relations for various square lattices (**f=0.72**). Solid lines are for TM waves and broken lines for TE waves.
(a) Circular cross-section of cavity (**r/a=0.48**).
(b) Rectangular cross-section of cavity (**d/a=0.85**).

Figs. 3(a) and 3(b) show additional dispersion relations for the square lattice with a circular cross-section (**r/a=0.48 in Fig. 3(a)**) and the square lattice with a rectangular cross-section (**d/a=0.85 in Fig. 3(b)**). When **r/a** and **d/a** have a high value, it is obvious that the two dispersion relations have distinct differences. Here, in the same way as above, we assumed the ideal filling factor of **0.72** in the two square lattices. In Fig. 3(a), we have wide PBG for the TM wave around the normalized frequency ($\omega a/2\pi c$) of 0.3 and there is no PBG for the TE wave in the case of square lattice with circular cross-section cavities. In Fig. 3(b), on the other hand, we have a very narrow PBG for the TM wave and wide PBG for the TE wave in the case of square lattice with rectangular cross-section cavities. In considering these results, there is the well-known general rule of thumb, in which a TM-mode PBG is apt to appear in a lattice of effectively-isolated dielectric regions and, likewise a TE-mode PBG is apt to appear in a lattice structure of un-isolated dielectric regions [2]. We can understand the mechanism to be as follows. Since the TE wave has the electric field assigned in x-y plane (see Fig. 1), the electric energy is easily stored in the un-isolated dielectric regions of the lattice. Since the TM wave has the electric field along the z direction (see Fig. 1), the electric energy is easily stored in the isolated dielectric regions of the lattice. Band gap is created when we have an energy difference between the stationary wave existing stationary in the material with a large averaged refractive index and the wave in a small averaged refractive index, which is realized at the boundaries of the corresponding Brillouin zone.

Figs. 4(a) and 4(b) illustrate examples of photonic crystal with a large filling factor. In

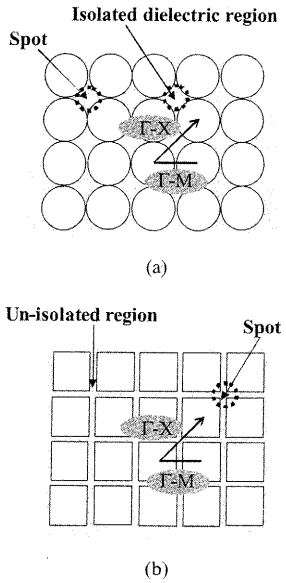

Fig.4 Illustrations of PCs having a large filling factor for various square lattices (f=0.72).
(a) Circular cross-section of cavity.
(b) Rectangular cross-section of cavity.

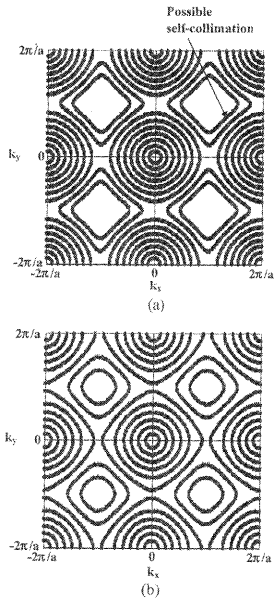

Fig.5 Equi-frequency contours for various square lattices (**f=0.72**).
(a) Circular cross-section of cavity (**r/a=0.48**).
(b) Rectangular cross-section of cavity (**d/a=0.85**).

Fig. 4(a), the lattice with a large cavity of circular cross-section is ready to leave behind isolated dielectric regions, while the lattice with a rectangular cross-section makes un-isolated dielectric regions, as shown in Fig. 4(b). This difference in the structure-dependent aspects of the two types of lattice results in a difference in dispersion relations and in PBGs, as shown in Figs. 3(a) and 3(b). In addition, the spot shape (Fig. 4) yields difference between the two dispersion relations. Since the spot is fabricated by Si surroundings with air cavities on silicon-on-insulator (SOI) substrate, most of the light-wave energy is stored inside the spot (Si) with a dielectric constant higher than that of the air cavities. The geometrical difference of spot shape brings out this difference of dispersion relations, even for the identical filling factor.

Aspects of dispersion relations of different cavity shape appear not only in the frequency range of PBG but also in equi-frequency contours. TE wave equi-frequency contours are plotted in Fig. 5: those for the lattice with a circular cross-section (**r/a=0.48**) are shown in Fig. 5(a) and those with a rectangular cross-section (**d/a=0.85**) in Fig. 5(b). Vertical and horizontal axes stand for wave number k_x and wave number k_y, respectively. Even for the identical filling factor (**f=0.72**), the line shape of equi-frequency contours for different cavity cross-sections shows a somewhat different aspect. It is expected that weak self-collimation of light waves will be observed for the square lattice with a circular cross-section of cavity (see Fig. 5(a)), but not for the lattice with a rectangular cross-section of cavity (see Fig. 5(b)).

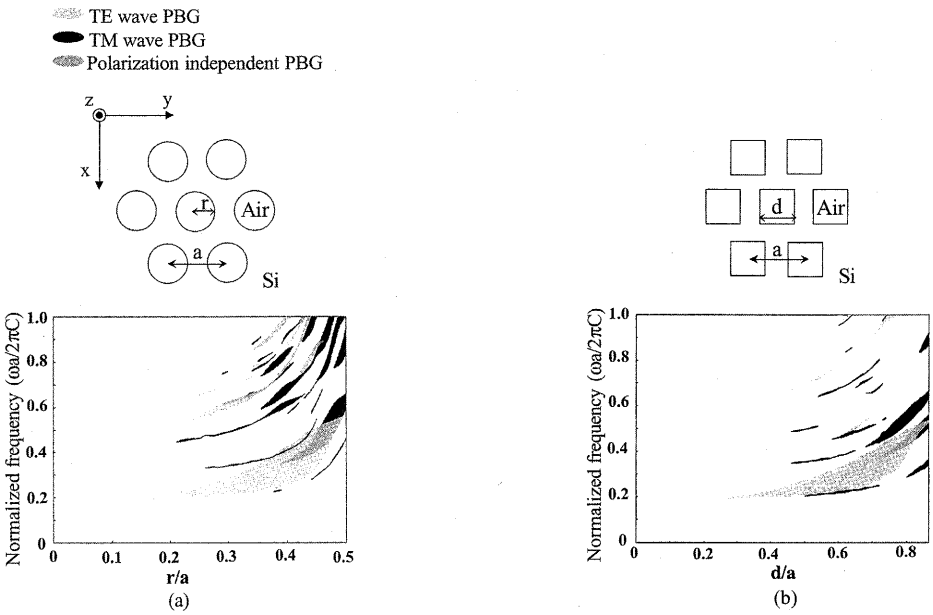

Fig.6 PBG map for various triangular lattices.
(a) Circular cross-section of cavity.
(b) Rectangular cross-section of cavity.

2.2 Triangular lattice

A triangular lattice with cavities of circular or rectangular cross-section is shown in Fig. 6. Parameter notations (**a, r** and **d**) are the same as those used in Fig. 1. We calculated dispersion relations of these photonic crystals for various **r/a** or **d/a** values. Fig. 6(a) shows the PBG map for the triangular lattice with cavities of a circular cross-section. The vertical axis shows the normalized frequency ($\omega a/2\pi c$). The horizontal axis shows the circular radius normalized by the lattice constant (**r/a**). As shown in Fig. 6(a), the circular cross-section cavity makes a wide TE-wave PBG; the TM-wave PBG is narrower than the TE-wave PBG. Fig. 6(b) shows the PBG map for the triangular lattice with a rectangular cross-section cavity. Vertical and horizontal axes stand for the normalized frequency ($\omega a/2\pi c$) and the rectangular cavity width normalized by the lattice constant (**d/a**). On comparing features of the two PBG maps, it may be seen that the TE-wave PBG for the lattice with a circular cross-section cavity has features similar to those for the lattice with a rectangular cross-section cavity; the TM-wave PBG for the lattice with a rectangular cross-section cavity is separated into two regions; and the polarization-independent PBG for the lattice with a circular cross-section cavity is wider than that for the lattice with a rectangular cross-section cavity. However, just like the square lattice, we can see a negligible difference of band structures between lattices with the two types of cavity shape for a small filling factor.

Now, we will turn to band-structure symmetry in a triangular lattice with cavities of a rectangular cross-section. The real-space triangular lattice is shown in Fig. 7(a), and the triangular lattice in the corresponding reciprocal space is shown in Fig. 7(b). In Fig. 7(a), material geometry along the vector $\vec{a}$ is different from that along vector $\vec{b}$, because cavity

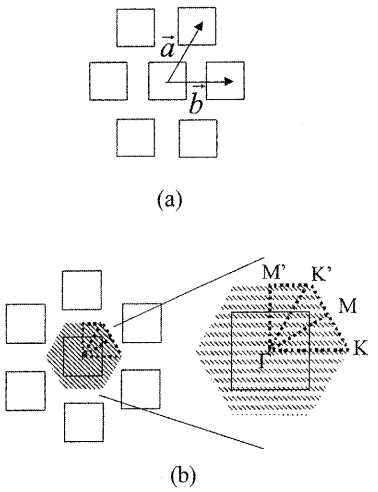

Fig.7 Illustrations of triangular lattice with a rectangular cross-section of cavity.
(a) Lattice illustrated in a real space.
(b) Reciprocal lattice and Brillouin zone.

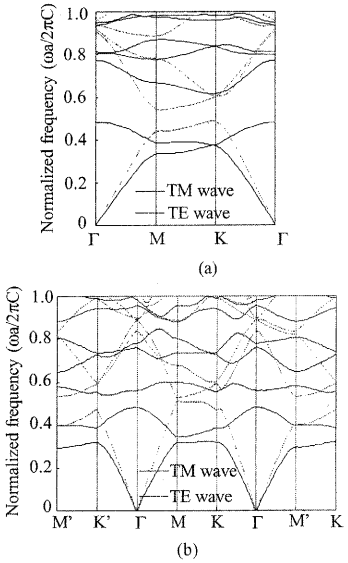

Fig.8 Dispersion relations for various triangular lattices **(f=0.83)**. Solid lines are for TM waves and broken lines for TE waves.
(a) Circular cross-section of cavity **(r/a=0.48)**.
(b) Rectangular cross-section of cavity **(d/a=0.85)**.

cross-section is rectangular in cross-section: This is a significant aspect of a triangular lattice with rectangular cavities. As a result, optical properties at points K' and M' in the first Brillouin zone are not equal to those at points K and M in the first Brillouin zone, as shown in Fig. 7(b). A triangular lattice with cavities of rectangular cross-section breaks band structure symmetry, but it still has the band structure symmetry of 120 degrees. On the other hand, a triangular lattice with cavities of circular cross-section has a band structure symmetry of 60 degrees.

As mentioned earlier in the context of a square lattice, when **r/a** or **d/a** has a small value, dispersion relations for both a triangular lattice with cavities of a rectangular cross-section and those for a triangular lattice with cavities of circular cross-section are very similar. When **r/a** or **d/a** has a small value, the difference in optical properties between points K' and M' of the first Brillouin zone and points K and M of the first Brillouin zone is not significant for a triangular lattice with cavities of rectangular cross-section.

When **r/a** or **d/a** has a large value, two dispersion relations show a somewhat different aspect. Figs. 8(a) and 8(b) illustrate calculated dispersion relations for a lattice with cavities of a circular cross-section **(r/a=0.48)** and for a lattice with cavities of a rectangular cross-section **(d/a=0.85)**, respectively. In Fig. 8, the filling factors of the two lattices are identical to each other **(f=0.83)**, but their dispersion relations have many different features. In Fig. 8(b), the TE-wave PBG along the M direction of the first Brillouin zone is narrow because of a rectangular cross-section cavity. Figs. 9(a) and 9(b) illustrate two different PC structures with a large filling factor. In Fig. 9(a), we can see isolated Si spots surrounded by air

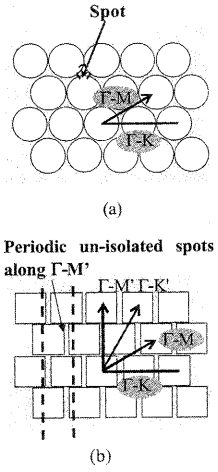

Fig.9 Illustrations of PCs having a large filling factor for various triangular lattices.
(a) Circular cross-section of cavity.
(b) Rectangular cross-section of cavity.

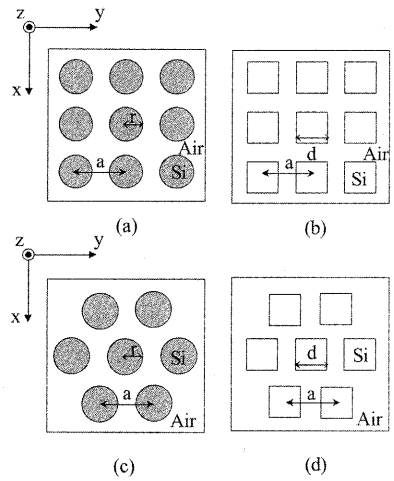

Fig.10 Illustrations of PCs for various lattice structures.
(a) Square lattice with pillars of a circular cross-section.
(b) Square lattice with pillars of a rectangular cross-section.
(c) Triangular lattice with pillars of a circular cross-section.
(d) Triangular lattice with pillars of a rectangular cross-section.

cavities aligned independently of crystal axis. In Fig. 9(b), there is no un-isolated spot along the Γ-M direction. So, since the TE-wave PBG is easily created for un-isolated spots, the TE-wave band gap along the Γ-M direction is narrow. In addition, the dispersion relation along the Γ-M direction is different from that along the Γ-M' direction, as shown in Fig. 8(b). In Fig. 9(b), the Γ-M' direction has periodic-un-isolated spots, and the TE-wave band gap along the Γ-M' direction is wider than the TE-wave band gap along the Γ-M direction. Wide perfect PBG exists for a circular cross-section cavity (see Fig. 8(a)), while narrow perfect PBG exists for a rectangular cross-section cavity (see Fig. 8(b)). This is caused by the difference in spot shape.

3. Periodic Silicon Pillar Array

Finally, we will discuss optical properties of lattices with Si pillar array. The PC structures with Si pillar array are shown in Fig. 10. Figs. 10 (a) and 10(b) are composed of square lattice, whereas Figs. 10(c) and (d) are of triangular lattice. Figs. 10(a) and 10(c) show PCs with a circular cross-section pillar and Figs. 10(b) and 10(d) show PCs with a rectangular cross-section pillar. Parameter values of **a**, **r** and **d** are the same as those used in Fig. 1 for square lattices and in Fig. 6 for triangular lattices. Fig. 11 shows the PBG maps for a square lattice with a circular cross-section pillar as a typical simulation result. The vertical axis represents the normalized frequency ($\omega a/2\pi c$). The transverse axis indicates the circular radius normalized by the lattice constant (**r/a**). For the Si pillar array, we can see only isolated Si regions, not un-isolated Si regions, but this depends on filling factor (**f**).

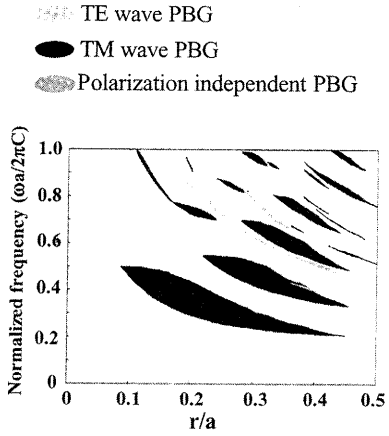

Fig.11 PBG maps for various lattices shown in Fig. 10(a).
A square lattice with pillars of a circular cross-section is assumed.

The TM-waves have a wide PBG, while the TE-waves have a narrow PBG. Since dielectric spots are made of air with a lower dielectric constant, the light wave energy is stored in Si pillars with a higher dielectric constant. In such cases, the effective permittivity of the PC region is ruled by silicon pillars. This suggests that simulation results for band structures of the PC structures shown in Fig. 10 will be almost identical to each other, regardless of pillar shapes. Actually, our simulation results do indicate the veracity of this prediction.

4. Conclusion

We investigated how the optical band structure of photonic crystal depends on lattice array structure (square lattice or triangular lattice) and cross-sectional shape of lattice point (circular or triangular shape). The band structures of PCs are categorized from the point of view of a PBG map. In lattices with air cavity array, when the filling factor is small, we see a slight difference of dispersion relations that arise independently of cavity shape. However, when the filling factor is large, it is clearly seen that the two dispersion relations have somewhat different aspects. In other words, the cross-section of the lattice-point modulates the band structure. A difference in the optical property of lattices with cavity or pillar of a circular or rectangular cross-section results not only in PBG aspect, but also in equi-frequency contours. For a triangular lattice, it was shown that the rectangular cross-section of lattice-point breaks the band structure symmetry. For lattices with an Si pillar array, we can see a slight difference of band structure between two-different pillar shapes because spots are made of air.

Acknowledgement

This study was financially supported by Kansai University Grant-in-Aid (Joint Research) 2003 and 2005.

References

1) R. A. Soref and J. P. Lorenzo, "All-silicon active and passive guided-wave components for λ =1.3 and 1.6 μm," *IEEE J. Quantum Electronics*, QE-22, p. 873 (1986).
2) J. D. Joannopoulos, R. D. Meade and J. N. Winn, 'Photonic crystals - Molding the flow of light,' Princeton University Press, Princeton, NJ, (1995).
3) K. Sakoda, "Optical properties of photonic crystals", Springer, New York, (2001).
4) E. Yablonovitch, "Inhibited spontaneous emission in solid-state physics and electronics," *Phys. Rev. Lett.*, 58, p. 2059 (1987).
5) A. Mekis, J. C. Chen, I. Kurland, S. Fan, P. R. Villeneuve and J. D. Joannopoulos, "High transmission through sharp bends in photonic crystral waveguides," *Phys. Rev. Lett.*, 77, p. 3787 (1996).
6) J. S. Foresi, P. R. Villeneuve, J. Ferrera, E. R. Thoen, G. Steinmeyer, S. Fan, J. D. Joannopoulos, L. C. Kimerling, H. I. Smith and E. P. Ippen, "Photonic-bandgap microcavities in optical waveguides," *Nature*, 390, p. 143 (1997).
7) T. Kinoshita, A. Shimizu, Y. Iida and Y. Omura, "Design senisitivity in quasi-one-dimensional silicon-based photonic crystalline waveguides," *J. Semicond. Tech. And Sci.*, 3, p. 55 (2003).
8) A. Polman, P. Wiltzius, T. A.Birks, E. Chow, V. L. Colvin, J. G.. Fleming, J. C. Knight, S. Lin, S. Noda, P. S. J. Russell, J. Schilling, W. L. Vos, A. J. Turberfield and R. B. Wehrspohn "MaterialsScience Aspects of Photonic Crystals," *MRS BULLETIN*, No. 8, 608 (2001).
9) X. Yu and S. Fan, "Bends and splitters for self-collimated beams in photonic crystals," *Appl.Phys. Lett.*, 83, p. 3251 (2003).
10) H. Kosada, T. Kawashima, A. Tomita, M. Notomi, T. Tamamura, T. Sato and S. Kawakami, "Superprism phenomena in photonic crystals," *Phys. Rev. B*, 58, p. 10096 (1998).
11) C. Luo, S. G. Johnson and J. D. Joannopoulos, "Subwavelength imaging in photonic crystals," *Phys. Rev. B*, 68, p. 0451151 (2003).
12) A. I. Cabuz, E. Centeno and D. Cassagne, "Superprism effect in bidimensional rectangular hotonic crystals," *Appl. Phys. Lett.*, 84, p.2031 (2004).
13) N. Susa, "Large absolute and polarization-independent photonic band gaps for various lattice structures and rod shapes," *J. Appl. Phys*, 91, p. 3501 (2002).
14) R. Wang, X. H. Wang, B. Y. Gu and G. Z. Yang, "Effects of shapes and orientations of scatterers and lattice symmetries on the photonic band gap in two-dimensional photonic crystals," *J. Appl. Phys*, 90, p. 4307 (2001).
15) C. Y. Hong, I. Drikis, S. Y. Yang, H. E. Horng and H. C. Yang, "Slab-thickness dependent bandgap size of two-dimensional photonic crystals with triangular-arrayed dielectric or magnetic rods," *J. Appl. Phys*, 94, p. 2188 (2003).
16) Y. Akahane, T. Asano, B. S. Song and S. Noda, "Investigation of high-Q channel drop filters using donor-type defects in two-dimensional photonic crystal slabs," *Appl. Phys. Lett.*, 83, p. 1512 (2003).
17) L. L. Lin, Z. Y. Li and K. M. Ho, "Lattice symmetry applied in transfer-matrix methods for photonic crystals," *J. Appl. Phys*, 94, p. 811 (2003).
18) R. L. Chern, C. C. Chang, C. C. Chang and R. R. Hwang, "Large full band gaps for photonic crystals in two dimensions computed by an inverse method with multigrid acceleration,"

Phys. Rev. E, 68, p. 0267041 (2003).

19) J. M. Hickmann, D. Solli, C.F. Mccormick, R. Plambeck and R.Y. Chiao, "Microwave measurements of the photonic band gap in a two-dimensional photonic crystal slab," *J. Appl.Phys*, 92, p. 6918 (2002).

20) X. Hu, Y. Shen, X. Liu, R. Fu and J. Zi, "Superlensing effect in liquid surface waves," *Phys. Rev. E*, 69, p. 0302011 (2004).

21) Y. Iida, Y. Omura, Y. Ogawa, T. Kinoshita and M. Tsuji, "Ring resonator with sharp u-turns using a SOI-based photonic crystal waveguide with normal single-missing-hole-line defect," *Proc. Of. SPIE*, 5277, p. 206 (2003).